Rhodamine 123 Binds to Multiple Sites in the Multidrug Resistance Protein (MRP1)†

Roni Daoud,‡ Christina Kast,§ Philippe Gros,§ and Elias Georges*,‡

Institute of Parasitology, Macdonald Campus, Ste-Anne-de-Bellevue, and Department of Biochemistry of McGill University, Quebec, Canada

Received August 31, 2000; Revised Manuscript Received October 10, 2000

ABSTRACT: The mechanisms of MRP1-drug binding and transport are not clear. In this study, we have characterized the interaction between MRP1 and rhodamine 123 (Rh123) using the photoreactive-iodinated analogue, [^{125}I]iodoaryl azido-rhodamine 123 (or IAARh123). Photoaffinity labeling of plasma membranes from HeLa cells transfected with MRP1 cDNA (HeLa-MRP1) with IAARh123 shows the photolabeling of a 190 kDa polypeptide not labeled in HeLa cells transfected with the vector alone. Immunoprecipitation of a 190 kDa photolabeled protein with MRP1-sepcific monoclonal antibodies (QCRL-1, MRPr1, and MRPm6) confirmed the identity of this protein as MRP1. Analysis of MRP1−IAARh123 interactions showed that photolabeling of membranes from HeLa-MRP1 with increasing concentrations of IAARh123 was saturable, and was inhibited with excess of IAARh123. Furthermore, the photoaffinity labeling of MRP1 with IAARh123 was greatly reduced in the presence of excess Leukotreine C_4 or MK571, but to a lesser extent with excess doxorubicin, colchicine or chloroquine. Cell growth assays showed 5-fold and 14-fold increase in the IC_{50} of HeLa-MRP1 to Rh123 and the Etoposide VP16 relative to HeLa cells, respectively. Analysis of Rh123 fluorescence in HeLa and HeLa-MRP1 cells with or without ATP suggests that cross-resistance to Rh123 is in part due to reduced drug accumulation in the cytosol of HeLa-MRP1 cells. Mild digestion of purified IAARh123-photolabeled MRP1 with trypsin showed two large polypeptides (∼111 and ∼85 kDa) resulting from cleavage in the linker domain (L1) connecting the multiple-spanning domains MSD0 and MSD1 to MSD2. Exhaustive proteolysis of purified IAARh123-labeled 85 and 111 kDa polypeptides revealed one (6 kDa) and two (∼6 plus 4 kDa) photolabeled peptides, respectively. Resolution of total tryptic digest of IAARh123-labeled MRP1 by HPLC showed three radiolabeled peaks consistent with the three *Staphylococcus aureus V8* cleaved peptides from the Cleveland maps. Together, the results of this study show direct binding of IAARh123 to three sites that localize to the N- and C-domains of MRP1. Moreover, IAARh123 provides a sensitive and specific probe to study MRP1−drug interactions.

Selection of tumor cell lines resistant to natural product toxins has been shown to result in the overexpression of either or both transmembrane proteins, P-glycoprotein (P-gp1)[1] and the multidrug resistance protein (MRP1) (*1*, *2*). Gene transfer studies using MRP1 cDNA into drug sensitive tumor cells have been shown to confer resistance to structurally dissimilar anti-cancer drugs and to other natural product toxins (*3*). The human MRP gene family consists of seven orthologs [MRP1−7; (*4*)], with MRP1, 2, and 3 shown to confer drug resistance when transfected into drug sensitive cells (*5*, *6*). The functions of the other members of the MRP gene family are less defined. MRP1 is a member of a large family of membrane-trafficking proteins (*7*) that couple ATP hydrolysis to the transport of diverse molecules across the cell membrane. Sequence analysis of MRP1 has predicted the presence of three membrane-spanning domains (MSD0, MSD1, and MSD2), and two nucleotide-binding domains (NBD1 and NBD2). The linear arrangement of MRP1 begins with a hydrophobic domain (MSD0) which is connected by a linker domain (L0) to an MDR1-like core (MSD1-NBD1-L1-MSD2-NBD2) (*7*−*10*). Unlike MSD1 and MSD2, which encode six transmembrane sequences each, MSD0 encodes five transmembrane sequences with an extracytoplasmic N-terminal (*9*, *10*). The role of MSD0 domain in MRP1 functions is not yet clear, however, deletion of the linker domain (L0) between MSD0 and MSD1 inhibits Leukotreine C_4 (LTC_4) transport (*11*, *12*).

MRP1 is expressed to varying levels in normal human tissues and is thought to mediate the transport of modified cell metabolites (*13*). Disruption of the *mrp1* gene in mice caused a significant increase in the accumulation of natural product toxins and glutathione in MRP1-expressing tissues (*14*−*16*). Although the normal functions of MRP1 are not entirely clear, Wijnholds et al. (*16*) have recently shown

† This work was supported by grants from the Natural Sciences and Engineering Research Council of Canada (NSERC) to E.G. and National Cancer Institute of Canada (NCIC) to P.G. Research at the Institute of Parasitology is partially supported by a grant from the FCAR pour l'aide à la recherche.

* To whom correspondence should be addressed. Phone: (514) 398 8137. Fax: (514) 398 7857. E-mail: elias_georges@maclan.mcgill.ca.

‡ Institute of Parasitology.

§ Department of Biochemistry of McGill University.

[1] Abbreviations: MDR, multidrug resistance; P-gp, P-glycoprotein; MRP1, multidrug resistance protein; SDS−PAGE, sodium dodecyl sulfate−polyacrylamide gel electrophoresis; Rh123, rhodamine 123; IAARh123, iodoaryl azido-rhodamine 123; ABC, ATP-binding cassette; MSD, membrane-spanning domain; NBD, nucleotide-binding domain.

10.1021/bi0020574 CCC: $19.00
Published on Web 11/17/2000

MRP1 to function in mediating inflammatory responses possibly through its transport of the glutathione conjugated eicosanoid, LTC_4. In addition to LTC_4, other molecules that are conjugated to glutathione, glucuronate and sulfate are also substrates for MRP1 (*17*−*20*). Interestingly, certain nonconjugated natural product drugs are co-transported with glutathione (*21*, *22*). Furthermore, glutathione transport into MRP1-enriched membrane vesicles was stimulated by vincristine (*21*, *22*).

The molecular mechanism by which MRP1 mediates resistance to natural product toxins is not well understood. However, there is considerable overlap between MRP1 and P-gp1 substrate specificity, which includes drugs from the *Vinca alkaloids* (vincristine), the anthracycline antibiotics (doxorubicin), the etoposides (VP16), and certain dyes (rhodamine 123) (*2*, *23*). Recent reports have demonstrated MRP1-mediated accumulation of unmodified *V. alkaloids* into membrane vesicles in the presence of high levels of GSH (*24*, *25*). On the basis of these results, it has been suggested that the drug binding domain of MRP1 is likely to be similar to that of Pgp1 (*26*); while the mechanism of drug efflux may be different and could require the catalytic presence and/or the co-transport of other molecules such as GSH. Earlier reports have demonstrated direct interaction between LTC_4 and MRP1 (*17*). Moreover, we have recently shown direct binding between MRP1 and two structurally different quinoline-based photoreactive drugs (*26*, *27*). In the latter study (*26*), MRP1 was photoaffinity labeled at multiple sites in the N- and C-terminal domains. The photoaffinity labeling of MRP1 with photoreactive drugs was inhibited in the presence of LTC_4 and MK571, known substrates of MRP1 (*26*, *27*). Thus while the findings of those studies suggest the same or overlapping sites in MRP1 for LTC_4 and unmodified quinoline-based drugs, it is not clear if previously identified photoaffinity labeled sites (*26*) are specific to quinoline-based drugs or represent sites in MRP1 that interact with other structurally diverse drugs. To address this possibility, it was of interest to study the interactions between MRP1 and rhodamine 123 (Rh123), xanthone-based drug, which is both structurally and functionally different from previously characterized quinoline-based drugs that interact with MRP1. Several studies have suggested that Rh123 is a substrate for MRP1 (*20*, *30*). However, it was not determined in those studies if Rh123 interacts with MRP1 (*20*, *30*). Interestingly, Rh123 is an excellent substrate for P-gp1 and its transport occurs by direct binding to P-gp1 (*28*−*31*). In this study, we report on the characterization of MRP1 interactions with Rh123 using the photoactive analogue IAARh123.

MATERIALS AND METHODS

Materials. Iodine-125 (100.7 mCi/ml) was purchased from Amersham Biochemical Inc., (Mississauga, Ontario, Canada). Protein A-sepharose was purchased from Pharmacia Inc. (Montreal, Quebec, Canada). Calcein AM was purchased from Molecular Probes Inc. (Eugene, OR). The LTD_4 receptor antagonist MK 571 was kindly provided by Dr. A. W. Ford-Hutchinson [Merck-Frost Centre for Therapeutic Research, Quebec, Canada (*32*)]. Leukotreine C_4 (LTC_4) was purchased from Cayman Chemical Co. (Ann Arbor, MI). All other chemicals were of the highest commercial grade available.

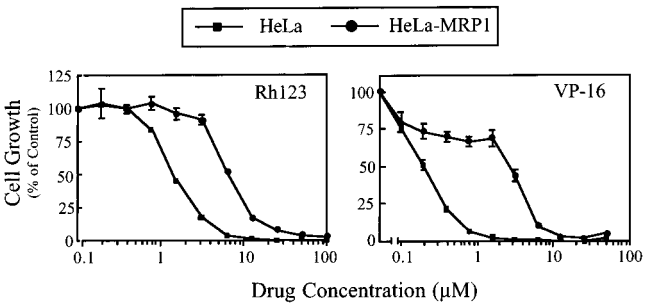

FIGURE 1: Effects of Rh123 and VP-16 on the growth of HeLa and HeLa-MRP1 cells. HeLa and HeLa-MRP1 cells were seeded at 2000 cells/well in 24-well plates and grown in the absence and the presence of increasing concentrations of Rh123 (0−100 μM) and the Etoposide, VP16 (0−50 μM). The viability of cells was estimated 6−7 days later by staining the surviving cell colonies with 0.1% methylene blue in 50% ethanol and (see Materials and Methods). Cell growth is expressed as percent of control in the absence of drug. Each point is the mean (± SD) of three independent experiments.

Cell Culture and Plasma Membrane Preparations. HeLa and HeLa-MRP1 transfectant cells were grown in α-MEM media containing 10% fetal calf serum (Hyclone) (*10*). HeLa-MRP1 cells were cultured continuously in the presence of 250 ng/mL etoposide (VP-16); however, cells used for drug transport studies were grown in drug-free media for several days prior to the date of the experiment. Plasma membranes from HeLa and HeLa-MRP1 cells were prepared as previously described (*10*). The resultant plasma membranes were further purified by sucrose gradient (*10*) and washed with 5 mM Tris-HCl, pH 7.4. Plasma membrane enriched fractions were resuspended in the same buffer with 250 mM sucrose. Membranes were stored at −80 °C if not immediately used. Protein concentrations were determined by the Lowry method (*33*).

Synthesis and Radio-Iodination of Photoreactive Rhodamine 123. A photoactive analogue of Rh123 (Iodoaryl azido-Rh123 or IAARh123) was synthesized by reacting Rh123 with NHS-ASA in DMF essentially as previously described (*28*). Briefly, 5 mg (16.5 μmol) of Rh123 was dissolved in DMF containing triethylamine. The mixture was added to 27 μmol of NHS-ASA in an equal volume of DMF. The reaction was allowed to proceed for 48 h at room temperature with constant agitation. The solvent was removed by vacuum-drying and the oily residue was dissolved in 250 μL of methanol. The photoactive derivative of Rh123, IAARh123 (Figure 4), was purified by high-performance liquid chromatography (HPLC) using a Vydac 201HS54 C_{18} reversed-phase column (4.6 mm × 25 cm) with a gradient of 20 to 100% acetonitrile in 0.025 M ammonium acetate buffer, pH 5.5. The reaction products were monitored at 505 or 290 nm. The HPLC peak corresponding to IAARh123 was further purified on the same column in the absence of UV detection to avoid photodestruction. IAARh123 was radio-iodinated as previously described (*28*).

Photoaffinity Labeling and Immunoprecipitation. Total membranes were incubated with 1 μM of IAARh123 in 20 μL of labeling solution (5 mM Tris, pH 7.4, 250 mM sucrose) for 30 min in the dark. Membranes were then incubated for an additional 10 min on ice followed by UV irradiation at 254 nm for 10 min while on ice (Stratgene 1800 UV cross-linker, Stratagene, La Jolla, CA). Following photoaffinity

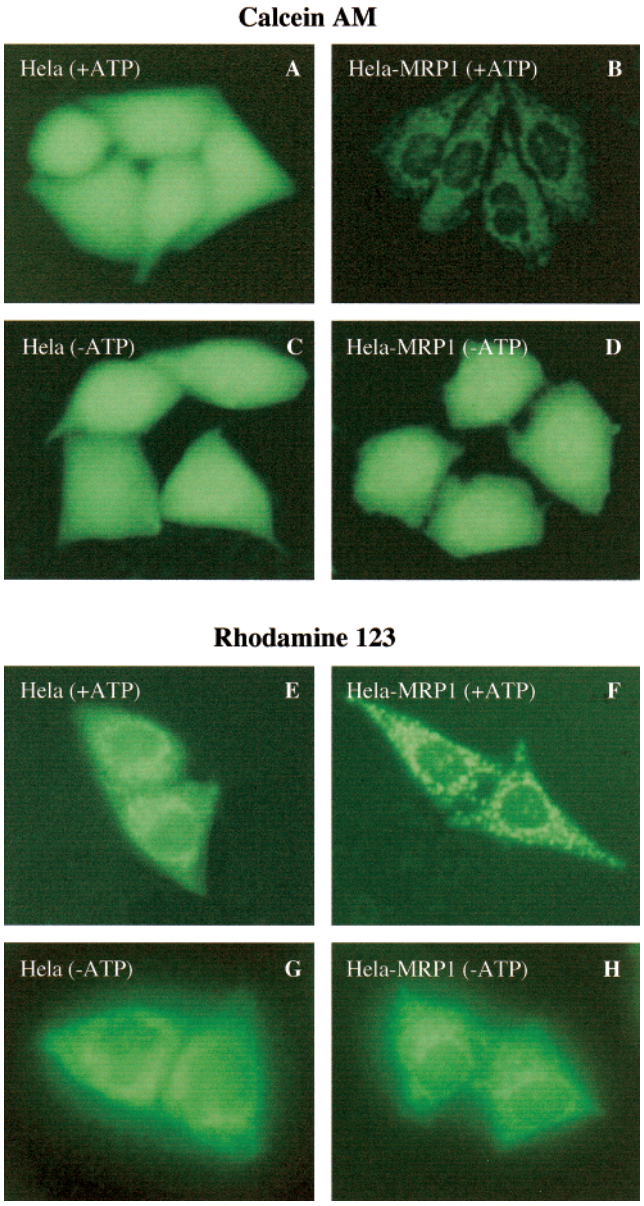

FIGURE 2: Rhodamine 123 and Calcein AM accumulation in HeLa and HeLa-MRP1 cells. Cells were incubated with Rh123 or Calcein AM at 37 °C in the presence of 10 mM D-glucose or 10 mM Deoxyglucose and 100 nM sodium azide. The fluorescence signals in HeLa and HeLa-MRP1 cells following the incubation of cells with Calcein AM under normal ATP levels (panels A and B) and ATP depleted levels (panels C and D). The same experiment was repeated with HeLa and HeLa-MRP1 cells incubated with Rh123 under normal ATP levels (panels E and F) and ATP-depleted levels (panels G and H). Cells were viewed at 400× magnification using Nikon TE200 inverted microscope equipped with a fluorescence filter.

labeling, samples were mixed with 80 μL of buffer A (1% SDS, 0.05 M Tris, pH 7.4) and 320 μL of buffer B (1.25% Triton X-100, 190 mM NaCl, 0.05 M Tris, pH 7.4). Immunoprecipitation was carried as previously described (*34*) using MRP1-specific monoclonal antibodies [QCRL-1, MRPm6 and MRPr1 (*35*)]. Immunoprecipitated proteins were resolved on SDS−PAGE using the Fairbanks system (*36*). Gels were dried and exposed to Kodak X-AR film at −80 °C. Alternatively, proteins were visualized by silver staining, using the NOVEX SilverXpress Silver Staining Kit.

Proteolytic Digestions and HPLC. The mild digestion of IAARh123-photolabeled MRP1 to obtain the 111 and 85 kDa

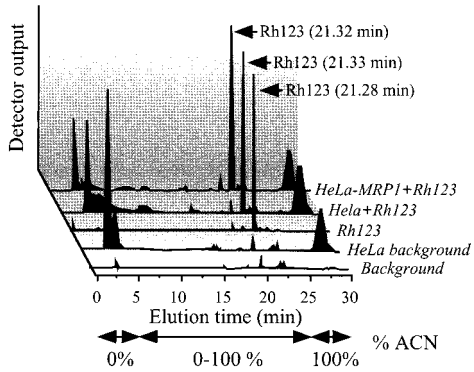

FIGURE 3: HPLC profile of Rh123 following incubation with HeLa and HeLa-MRP1 cells. Rh123 was extracted from HeLa and HeLa-MRP1 cell lysates (see Materials and Methods) following an incubation of cells at 37 °C. The mobility of Rh123 extracted from cells was compared to unmodified Rh123. Other controls included extracts from HeLa cells without exogenously added Rh123 and solvent controls. All samples were analyzed by HPLC using a Vydac column with C_{18} resin. A gradient of 0−100% acetonitrile (ACN) was used to elute Rh123.

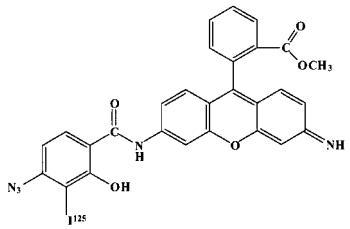

FIGURE 4: The organic structure of the photoactive analogue of Rh123 (or IAARh123).

polypeptides was accomplished as follows. IAARh123-photolabeled MRP1 was immunoprecipitated with the QCRL-1 Mab. MRP1/QCRL-1 complex bound to Protein A-Sepharose was then digested at 37 °C for 5 min with low concentrations of trypsin (8 or 16 ng/sample). Digestion was stopped with the addition of protease inhibitors (10 μg/mL leupeptin, pepstatin A, aprotinin, and 1 mM PMSF). The digested products of IAARh123-photolabeled MRP1 were eluted from Protein A-Sepharose at 65 °C in SDS−PAGE sample buffer. MRP1 fragments were resolved on Fairbanks gels, transferred to a nitrocellulose membrane and probed with MRPm6 and MRPr1 Mabs. The same membrane was also exposed to X-ray film to determine the relative positions of the IAARh123-photolabeled tryptic fragments. Alternatively, the two resulting polypeptides (the 85 and 111 kDa fragments) were immunoprecipitated separately with MRPr1 and MRPm6 Mabs. Briefly, HeLa-MRP1 membranes were photolabeled with IAARh123 and subjected to mild trypsin digestion (1:125 w/w) for 40 min. The digestion was stopped with a solubilization buffer (1% SDS, 0.05 M Tris, pH 7.4) containing an excess of protease inhibitors. The trypsin treated sample was divided in two halves and mixed separately with either MRPr1 or MRPm6 for immunoprecipitation as previously described (*26*). Immuno-purified IAARh123-photolabeled MRP1 or its fragments were resolved on Fairbanks gels and the resulting photolabeled polypeptides were exhaustively digested with *Staphylococcus aureus* V8 protease (20 μg/gel slice) in the wells of a 15% Laemmli gel according to the method of Cleveland et al. (*37*). For a complete tryptic digestion, IAARh123-photolabeled and immunopurified MRP1 was incubated with trypsin

(1:5 w/w) for 14 h at 37 °C. Digested samples were vacuum-dried and resuspended with 250 μL of 1% trifluoroacetic acid/water and resolved by reversed-phase HPLC (Vydac 201HS54 C_4 reversed-phase column). The chromatographic procedure consisted of an 80 min gradient of 0 to 100% acetonitrile with 1% trifluoroacetic acid at a flow rate of 1 mL/min. Fractions were collected and checked for radioactivity.

Accumulation of Calcein AM and Rhodamine 123. HeLa and HeLa-MRP1 cells, seeded in 60 mm dishes (1×10^5 cells/dish), were washed three times with Dulbecco's phosphate buffered salt solution and incubated (45 min, 37 °C) with 10 mM glucose or 10 mM deoxyglucose and 100 nM NaN_3. Rh123 or Calcein AM were added to a final concentration of 1 μM and cells were incubated for an additional 30 min. Cells were washed with ice cold Dulbecco's phosphate-buffered salt solution and observed using a Nikon TE200 inverted microscope equipped with a B-2A fluorescence filter.

Modification of Rhodamine 123 in Cells. To determine if Rh123 is metabolically modified in HeLa or Hela-MRP1 transfectants, cells were incubated with or without 1 μM of Rh123 for 1 h at 37 °C. Cells were washed with ice cold phosphate buffer, harvested, and lysed in 100 μL of 50mM Tris-HCl (pH 7.4), containing 2 mM $MgCl_2$ and 1% NP40. The cell extracts were centrifuged at 14000*g* for 5 min prior to the addition of 900 μL of cold methanol to the supernatant. The mixture was left overnight at −20 °C and then cleared by centrifugation at 14000*g* for 30 min. The supernatant was carefully removed and analyzed by HPLC using a Vydac 201HS54 C_{18} reversed-phase column. The chromatographic separation consisted of an aqueous phase of 0.025 mM ammonium acetate, pH 5.5, and 0 to 100% acetonitrile gradient. Elution was monitored at 505 nm.

Cytotoxicity Assays. HeLa and Hela-MRP1 transfectants were seeded at 2000 cells/well in 24-well plates. Cells were allowed to grow overnight prior to the addition of drugs at increasing concentrations. Cells were grown for 6−7 days and then stained with 0.1% methylene blue in 50% ethanol as previously described (*38*). The staining of adherent cells was extracted by incubating stained cells with 250 μL of 0.1% SDS in phosphate-buffered saline solution at 37 °C for 1 h with shaking. The released stain from each well was quantified at 570 nm using a Dynatech MR5000 plate reader. The effects of drugs on the viability of cells were expressed as the mean ± standard deviation of three independent experiments in which triplicates were assayed.

RESULTS

Rhodamine 123, a cationic fluorescent dye, has been shown to accumulate selectively in the mitochondria of eukaryotic cells (*39*). Earlier studies have shownP-gp1 to mediate the transport of Rh123 by direct binding (*28*, *40*). In this study, it was of interest to learn if MRP1 also mediates Rh123 transport via direct binding. Figure 1 shows the growth of HeLa and HeLa-MRP1 cells in the presence of increasing concentrations of Rh123 or the etoposide VP16. The results of Figure 1 show the IC_{50} of HeLa-MRP1 to be ∼14- and ∼5-fold higher than HeLa cells for VP16 and Rh123, respectively. These results are consistent with earlier observations by Zaman et al. (*20*), which demonstrated cross-resistance to Rh123 in MRP1 transfected SW1573 cells. However, the latter study did not determine if Rh123 is transported by MRP1 (*20*). Figure 2 shows the accumulation of Rh123 and Calcein AM in HeLa and HeLa-MRP1 with and without ATP. The results in Figure 2 (panels A and B) show large decrease in Calcein AM accumulation in HeLa-MRP1 versus HeLa cells. Moreover, inhibition of ATP levels resulted in increased Calcein AM fluorescence in HeLa-MRP1 cells to the same level as HeLa cells (panel C versus D). A less dramatic decrease was observed for Rh123 accumulation in HeLa-MRP1 versus HeLa cells (Figure 2, panels E and F). Thus while both cell lines (HeLa-MRP1 and HeLa) showed intracellular Rh123 fluorescence, HeLa-MRP1 showed less diffused fluorescence in the cytoplasm as compared to HeLa cells (Figure 2, panel E and F). Interestingly, this difference in Rh123 fluorescence between HeLa-MRP1 and HeLa cells ceased when ATP synthesis in both cell lines was inhibited with 100 nM sodium azide and 10 mM deoxyglucose (Figure 2, panel G and H).

It is presently believed that conjugation of certain compounds to anionic moieties (glutathione, sulfate, and glucuronic acid) may be required for their transport by MRP1. To determine if modification of Rh123 is required for its interaction with MRP1 and transport in intact cells, HeLa and HeLa-MRP1 cells were incubated with 1 μM of Rh123 for 1 h at 37 °C and then the status of Rh123 was compared to unmodified Rh123 by HPLC. The chromatograms in Figure 3 show the elution time of Rh123 incubated with HeLa or HeLa-MRP1 to be identical to that of control unmodified Rh123. Therefore collectively, the results in Figures 1−3 demonstrate clearly that modification of Rh123 is not required for its transport from MRP1-expressing cells.

To address the question of whether MRP1 interacts directly with unmodified drugs in a fashion similar to Pgp1, we examined the binding of Rh123 to MRP1 in HeLa-MRP1 transfectant cells. To demonstrate a direct binding of MRP1 to Rh123, a photoactive radioiodinated analogue of Rh123 (IAARh123; Figure 4) was synthesized as previously described (*28*) and used to photolabel MRP1 in membrane-enriched fractions from HeLa and HeLa-MRP1. The results in Figure 5a (lanes 3 and 4) show the labeling of membranes from HeLa and HeLa-MRP1 cells by IAARh123, respectively. A 190 kDa protein in HeLa-MRP1 but not in HeLa cells was photoaffinity labeled by IAARh123. Lanes 1 and 2 of Figure 5A show total membrane proteins resolved on SDS−PAGE and stained by silver staining, indicating that the 190 kDa is photolabeled to much higher levels than other highly expressed proteins (ca. 28−60 kDa). Thus the labeling of the 190 kDa by IAARh123 is not due to its high expression and therefore it is selectively labeled. To confirm the identity of the 190 kDa protein as MRP1, HeLa and HeLa-MRP1 membranes were photoaffinity labeled with IAARh123 and then immunoprecipitated with an MRP1-specific monoclonal antibody, QCRL-1 (Figure 5B, lanes 3 and 4). Lane 4 shows a single polypeptide with an apparent molecular mass of 190 kDa that is not immunoprecipitated from HeLa membranes. Similar immunoprecipitations of IAARh123-photolabeled membranes with an irrelevant IgG_{2a} did not precipitate a 190 kDa protein (lanes 1 and 2 of Figure 5B). To determine the photolabeling specificity of MRP1 by IAARh123, membranes from HeLa-MRP1 cells were photolabeled with increasing concentrations of IAARh123

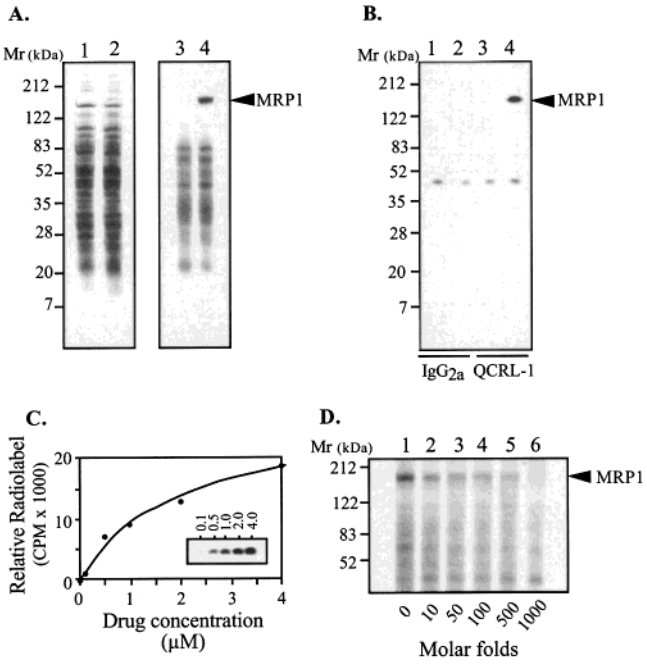

FIGURE 5: Photoaffinity labeling of MRP1 by IAARh123. Plasma membranes from drug sensitive (HeLa) and resistant (HeLa-MRP1) cells were photoaffinity labeled with IAARh123 and resolved on SDS−PAGE (lanes 3 and 4 of panel A). Lanes 1 and 2 of panel A show the staining of membrane proteins from HeLa and HeLa-MRP1 by Silver staining. Panel B shows IAARh123-photoaffinity labeled membranes from HeLa and HeLa-MRP1 cells immunoprecipitated with MRP1-specific Mab (QCRL-1) (lanes 3 and 4) or an irrelevant IgG_{2a} (lanes 1 and 2). Panel C shows the photoaffinity labeling of HeLa-MRP1 membranes with increasing concentrations of IAARh123 (0−4.0 μM). The inset in panel C shows the increase in the intensity of a 190 kDa photolabeled protein, which was excised, and the radioactivity quantified. Panel D shows the photolabeled membranes from HeLa-MRP1 cells incubated in the absence or presence of excess (0.1−100 μM) IAARh123.

(0.1−4 μM) or in the presence of increasing molar concentrations of IAARh123 (Figure 5, panels C and D, respectively). The results in Figure 5C show saturable photolabeling of MRP1 at higher concentrations of IAARh123. Similarly, photolabeling of MRP1-enriched membranes with IAARh123 in the presence of an increasing molar excess of IAARh123 showed a dramatic decrease in the photolabeling of MRP1 (Figure 5D). Taken together, the results in Figure 5 show a direct and specific photoaffinity labeling of MRP1 by IAARh123. Similar labeling results were obtained using membranes from other MRP1 expressing cells, such as H69/AR or HL60/AR (data not shown).

To determine if IAARh123 binds to physiologically relevant site(s) in MRP1, membranes from HeLa-MRP1 cells were photolabeled with IAARh123 in the presence of molar excess of colchicine, chloroquine, doxorubicin, MK571, and LTC_4. The photoaffinity labeling of MRP1 was inhibited at 160-fold molar excess of LTC_4 (Figure 6A). Similarly, molar excess (150-fold) of MK 571 caused a significant decrease in the photolabeling of MRP1 by IAARh123. Colchicine, chloroquine, and doxorubicin at 1000-fold molar excess were less effective than LTC_4 or MK571 (Figure 6A). Interestingly, molar excess of Calcein AM, which is transported by MRP1, showed a significant inhibition of IAARh123 photolabeling of MRP1 (Figure 6C). Calcein AM at 125-fold

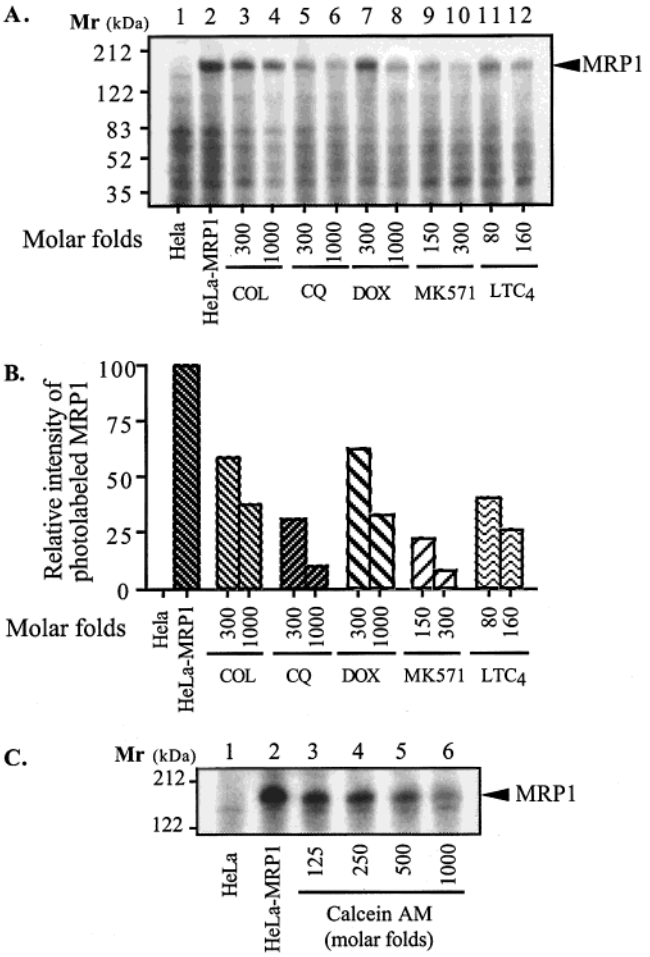

FIGURE 6: Effects of diverse drugs on the photoaffinity labeling of MRP1 by IAARh123. HeLa or HeLa-MRP1 cells were photoaffinity labeled with IAARh123 in the absence or presence of molar excess (300−1000-fold) of Colchicine (COL), Chloroquine (CQ), Doxorubicin (DOX), MK571 (150−300), and LTC_4 (80−160). Panel 6B shows a plot of the relative decrease in the photolabeling of MRP1 with IAARh123 in the presence of the above drugs. Panel C shows the photolabeling of HeLa-MRP1 membranes by IAARh123 in the absence (lane 2) and in the presence of increasing molar concentrations (125−1000) of Calcein AM (lanes 3−6). Lane 1 shows the photolabeling of HeLa membranes with IAARh123.

molar excess inhibited more than 50% of MRP1 photolabeling by IAARh123. Further increase in Calcein AM concentrations resulted in greater inhibition of MRP1 photolabeling (Figure 6C, lanes 3−6). Consequently, these results show Rh123 to interact with MRP1 at the same or overlapping site(s) as Calcein AM. Together, these results confirm the specificity of IAARh123 toward MRP1 and suggest that IAARh123 binding to MRP1 occur at the same or overlapping site(s) as MK 571 and LTC_4.

Studies of MRP1 topology using epitope insertion are consistent with the predicted model of MRP1 (Figure 7A), which suggests the presence of an extracytoplasmic N-terminal with MSD0-L0 plus an MDR1-like core of MSD1-NBD1-L1-MSD2-NBD2 (*8*−*10*). Moreover, biochemical analysis of MRP1 has demonstrated the presence of two trypsin sensitive sites within the two linker domains (L0 and L1; Figure 7A) that connect MSD0 to MSD1 + MSD2 and MSD0 + MSD1 to MSD2 sequences (*26*, *41*). Treatment of MRP1 enriched membranes with limiting amounts of trypsin results in the cleavage at L1 sequence followed by a second

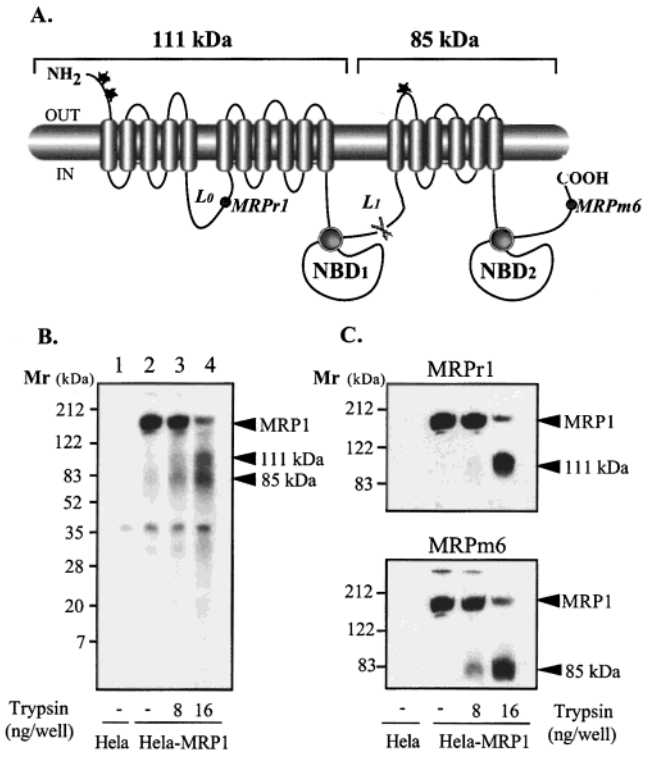

FIGURE 7: Photoaffinity labeling of two large polypeptides of MRP1 by IAARh123. MRP1 photoaffinity labeled by IAARh123 was purified from HeLa-MRP1 membranes and subjected to mild tryptic digestion. The photolabeled-radiolabeled products were resolved by SDS−PAGE (panel B) and transferred to nitrocellulose exposed to X-ray film and then processed for Western blotting (panel C). Panel B shows the signal from purified IAARh123 photolabeled MRP1 incubated in the absence and in the presence of 8 and 16 ng of trypsin, respectively. Panel C shows the Western blot of the IAARh123 photolabeled MRP1 tryptic digest probed separately with MRPr1 and MRPm6 Mabs. Panel A shows a schematic of MRP1 predicted topology with the above two Mabs epitopes in MRP1 relative to the protease hypersensitive sites in L0 and L1. The nucleotide binding domains (NBD1 and NBD2) and the extracellular glycosylation sites (**) are indicated on the schematic of MRP1 secondary structure (panel A).

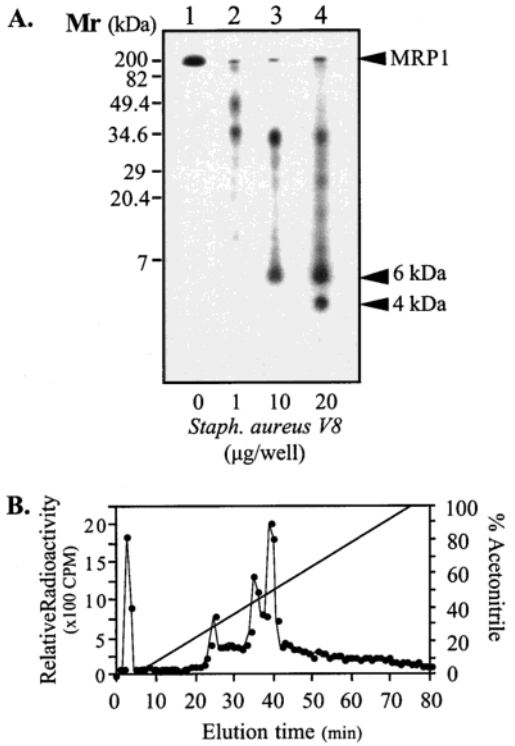

FIGURE 8: Complete proteolytic digestion of IAARh123-photoaffinity labeled MRP1. Purified MRP1 photoaffinity labeled with IAARh123 was subjected to complete in-gel or solution digestions. The in-gel digested MRP1 products were resolved on 15% acrylamide SDS−PAGE, while the solution digested products were resolved by reverse-phase chromatography. Lanes 1−3 of panel A show an in-gel digestion of IAARh123-photolabeled MRP1 with increasing concentrations of *S. aureus V8* (1−20 μg/well). Figure 8B shows the separation of MRP1 photoaffinity labeled tryptic peptides on a C_{18} reversed-phase column using 0 to 100% gradient of acetonitrile. The amount of radiolabel in each eluted fraction was plotted versus time. The peak signal at the beginning of the gradient represents the void volume.

cleavage at L0 (*41*). Earlier studies have shown that cleavage at L1 generates two fragments of 120 kDa and 75−80 kDa polypeptides containing MSD0-MSD1-NBD1 and MSD2-NBD2, respectively (*8*−*10*, *26*). Figure 7B shows such a limited trypsin digestion of IAARh123-photolabeled MRP1. Lanes 3 and 4 of Figure 7B show two photoaffinity labeled polypeptides (111 and 85 kDa), consistent with the predicted trypsin cut at L1. To confirm the identity of MRP1 tryptic fragments, tryptic digest of IAARh123-photolabeled MRP1 was analyzed by Western blotting with two epitope-specific monoclonal antibodies MRPr1 and MRPm6, which bind to sequences in the 111 kDa and the 85 kDa fragments, respectively. Figure 7C shows Western blots of the same samples as in Figure 7B probed with MRPr1 and MRPm6 Mabs, respectively. The results in Figure 7C show clearly that MRPm6 recognizes the 85 kDa polypeptide, while MRPr1 recognizes the 111 kDa fragment. Accordingly, the limited trypsin digestion of MRP1 is consistent with earlier proteolysis profiles of MRP1 confirming the identity of the 85 kDa and the 111 kDa polypeptides as MRP1 sequences containing MSD0-MSD1-NBD1 and MSD2-NBD2, respectively. In addition, photoaffinity labeling of both polypeptides with IAARh123 suggests the presence of at least one photolabeled site in each fragment of MRP1.

Our earlier report using a quinoline-based photoreactive drug (IACI) demonstrated the photoaffinity labeling of three tryptic peptides in MRP1 (*26*). To determine the number of IAARh123-photolabeled sites in MRP1, photoaffinity labeled MRP1 was purified with QCRL-1 Mab and subjected to in-gel digestion with increasing concentrations of *S. aureus* V8 protease (1−20 μg/gel slice). Figure 8A shows the resultant proteolytic fragments migrating with apparent molecular masses of 6 and 4 kDa. Similarly, purified IAARh123-photolabeled MRP1 was subjected to exhaustive trypsin digestion and the resulting digest was resolved by HPLC using reversed-phase chromatography. Figure 8B shows the IAARh123-photolabeled tryptic peptides resolved on a C_4 reversed-phase column with 0−100% acetonitrile gradient. The results in Figure 8B show three peaks eluting between 30 and 50% acetonitrile. Hence, by contrast to the exhaustive V8 digestion, the tryptic digestion suggests the presence of three photolabeled peptides. To identify the origin of the 4 kDa and 6 kDa labeled peptides relative to the two large photolabeled domains of MRP1, IAARh123-photolabeled 111 and 85 kDa polypeptides were purified and digested exhaustively with *S. aureus* V8 protease. Lanes 2 and 3 of Figure 9A show IAARh123-photolabeled 111 and 85 kDa

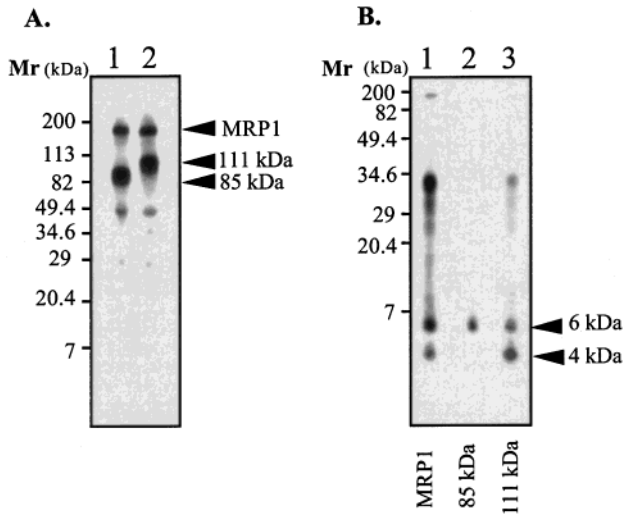

FIGURE 9: Proteolytic cleavage of immunopurified IAARh123-photolabeled N- and C-halves of MRP1. MRP1 enriched membranes were photolabeled with IAARh123 and subjected to mild tryptic cleavage. Lanes 1 and 2 of Figure 9A show mild trypsin-digest of MRP1 the immunoprecipitated with MRPm6 and MRPr1 Mabs, respectively. The resulting immunopurified IAARh123 photolabeled 111 and 85 kDa polypeptides from Figure 9A were excised from the gel and digested exhaustively with *S. aureus V8* (Figure 9B). Lanes 1−3 of Figure 9B show the resulting IAARh123-photolabeled peptides following in-gel digestion of MRP1, 111 and 85 kDa polypeptides with *S. aureus V8*.

polypeptides following immunoprecipitation with MRPr1 and MRPm6 Mabs, respectively. Exhaustive digestion of the 111 kDa polypeptide, which corresponds to MSD0-MSD1-NBD1 of MRP1, resulted in two photolabeled peptides migrating with apparent molecular masses of 4 and 6 kDa (Figure 9B). Similarly, digestion of the 85 kDa polypeptide, which corresponds to MSD2-NBD2 of MRP1, resulted in only one photolabeled peptide of 6 kDa (Figure 9B). Collectively, the results in Figure 9 suggest the presence of three IAARh123-labeled peptides in MRP1.

DISCUSSION

We have previously used two photoreactive quinoline derivatives to demonstrate direct and specific binding to MRP1 (*26*, *27*). Using these photoreactive drugs we demonstrated that modification with glutathione, glucuronate, or sulfate was not required for binding to MRP1 (*26*, *27*). In this report, we have synthesized a photoreactive drug analogue of Rh123 (IAARh123) and demonstrated the photoaffinity labeling of a 190 kDa protein or MRP1. The identity of the 190 kDa photolabeled protein as MRP1 was confirmed by its reactivity with three MRP1-specific Mabs [QCRL-1, MRPr1, and MRPm6 (*41*)]. The binding specificity of IAARh123 to physiologically relevant site(s) in MRP1 was confirmed by competitive inhibition studies whereby molar excess of LTC_4 and MK571, known MRP1 substrates, inhibited the photoaffinity labeling of MRP1 by IAARh123. By contrast, higher concentrations of natural product toxins (colchicine, chloroquine and doxorubicin) were required to inhibit MRP1 photolabeling by IAARh123. It is not entirely clear why differences in the capacity of these drugs to inhibit MRP1 photoaffinity labeling exist, especially since both chloroquine and MK571 are quinoline derivatives. Using two different epitope-specific Mabs (MRPr1 and MRPm6), we demonstrated that mild proteolysis of membranes containing MRP1 produced a 111 and 85 kDa polypeptides corresponding to MSD0-MSD1-NBD1 and MSD2-NBD2, respectively. Similar proteolysis of IAARh123-photolabeled MRP1 showed both fragments (111 and 85 kDa) to be photolabeled. However, exhaustive digestion of IAARh123 with trypsin revealed three radiolabeled peptides by HPLC. Analysis of the three IAARh123 photolabeled peptides showed the 111 kDa fragment to contain ∼4 and ∼6 kDa photolabeled peptides while the 85 kDa fragment contained only the ∼6 kDa photolabeled peptide. These results are interesting since similar peptides were photoaffinity labeled with IACI, a structurally dissimilar photoreactive quinoline-derived drug (*26*); suggesting the presence of common drug binding domain(s) that include the three photolabeled peptides of MRP1. It is interesting that photolabeling of P-gp1 with several P-gp1-specific photoreactive drugs produced two photolabeled peptides ca. 4 and 7 kDa peptides (*28*, *42*, *43*). Indeed photoaffinity labeling of P-gp1 with IAARh123 led to the photolabeling of the latter two peptides in P-gp1 (*28*). Further analysis of P-gp1 photolabeled peptides localized the two peptides to transmembrane 5−6 and 11−12 in MSD1 and MSD2, respectively (*44*, *45*). Later mutational analyses of P-gp1 transmembranes 5−6 and 11−12 confirmed the relevance of these two domains in P-gp1-mediated drug binding and resistance (*46*, *47*). Although it is presently not clear what sequences in MRP1 encode for the photolabeled peptides, it is tempting to speculate that each of the photolabeled peptides corresponds to sequences found in one of the three multiple spanning domains (i.e., MSD0, MSD1, and MSD2). In support of the latter speculations, mutations of charged amino acid (Glu^{1208}−Gln and Arg^{1206}−Met) in TM16 of rat MRP2 resulted in the loss of transport activity for glutathione, glucuronate and sulfate conjugates (*48*). Thus, the 6 kDa IAARh123-photolabeled peptide that is found in the C-terminal half of MRP1 could represent any of the transmembrane sequences in MSD2. Analysis of MSD2 sequences for all possible V8 peptides showed a ∼6 kDa stretch that includes the sequences of transmembranes 16 and 17. In another study (*49*), substitution of the carboxyl third of human MRP1 with that of mouse *mrp*1 modulated MRP1 specificity to doxorubicin, whereas the LTC_4 transport was unaffected. Hence, these results support our findings with regards to the notion of more than one drug binding site in MRP1 and that at least one site is localized in the C-terminal portion of MRP1.

The ability of IAARh123 to photolabel MRP1 and P-gp1 (*28*) specifically and at physiologically relevant sites is interesting since the two proteins share only 15% sequence identity (*50*). Comparison between Rh123 binding sequences from MRP1 and P-gp1 should increase our understanding of the molecular mechanism of interactions between MRP1 or Pgp1 and drugs. Efforts are ongoing to obtain higher resolution mapping of IAARh123-photolabeled peptides.

Membrane transport systems containing MRP1 have been shown to mediate the accumulation of several normal cell metabolites and other cytostatic compounds that are derivatized with GSH, sulfate or glucuronate (*19*, *24*, *51*). However, it has not been possible to show clear transport of nonderivatized natural product toxins in membranes containing MRP1 in the absence of GSH (*19*, *24*, *51*). Thus, energy dependent transport of vincristine was shown only in the presence of

GSH (*21*). We have previously demonstrated reduced accumulation of unmodified chloroquine and other quinoline-derived drugs in two different MRP1 expressing tumor cells (*52*). The results in Figure 2 of this study show clearly that HeLa-MRP1 cells are capable of energy-dependent accumulation of Calcein AM while Rh123 is less efficiently transported. These findings are surprising since both Calcein AM and Rh123 are structurally similar, sharing the xanthone backbone. Indeed the results in Figure 6C show that both Rh123 and Calcein AM compete for the same or overlapping drug binding site(s). However, unlike Calcein AM, Rh123 carries two cationic charges at physiological pH that may influence its ability to be transported but not its interactions with MRP1. In an earlier study by Twentyman et al. (*53*), MRP1-expressing cells showed 70% clearance of Rh123 following a 2 h incubation. Alternatively, the inefficient transport of Rh123 by MRP1, in contrast to P-gp1, may be due to the requirement of other rate-limiting ligands. This speculation is consistent with the conclusion from an earlier study (*54*) whereby depolarization of the membrane potential by genistein accelerated the efflux of Rh123 in MRP1 expressing cells.

In conclusion, the findings of this study demonstrate clearly that Rh123 interacts directly and specifically with MRP1. Moreover, IAARh123 represents an excellent photoreactive compound that can be used to probe MRP1 and P-gp1 interactions with drugs. In addition, unlike other P-gp1 and MRP1 photoreactive probes, IAARh123 can be iodinated and is fluorescent.

REFERENCES

1. Ling, V. (1997) *Cancer Chemother. Pharmacol. 40* (Suppl.), S3−S8.
2. Cole, S., and Deeley, R. (1998) *Bioessays 20*, 931−940.
3. Grant, C. E., Valdimarsson, G., Hipfner, D. R., Almquist, K. C., Cole, S. P., and Deeley, R. G. (1994) *Cancer Res. 54*, 357−361.
4. Borst, P., Evers, R., Kool, M., and Wijnholds, J. (1999) *Biochim. Biophys. Acta 1461*, 347−357.
5. Kool, M., van der Linden, M., de Haas, M., Scheffer, G. L., de Vree, J. M., Smith, A. J., Jansen, G., Peters, G. J., Ponne, N., Scheper, R. J., Elferink, R. P., Baas, F., and Borst, P. (1999) *Proc. Natl. Acad. Sci. U.S.A. 96*, 6914−9619.
6. Zeng, H., Bain, L. J., Belinsky, M. G., and Kruh, G. D. (1999) *Cancer Res. 59*, 5964−5967.
7. Klein, I., Sarkadi, B., and Varadi, A. (1999) *Biochim. Biophys. Acta 1461*, 237−262.
8. Bakos, E., Hegedus, T., Hollo, Z., Welker, E., Tusnady, G. E., Zaman, G. J., Flens, M. J., Varadi, A., and Sarkadi, B. (1996) *J. Biol. Chem. 271*, 12322−12326.
9. Hipfner, D. R., Almquist, K. C., Leslie, E. M., Gerlach, J. H., Grant, C. E., Deeley, R. G., and Cole, S. P. C. (1997) *J. Biol. Chem. 272*, 23623−23630.
10. Kast, C., and Gros, P. (1997) *J. Biol. Chem. 272*, 26479−26487.
11. Gao, M., Yamazaki, M., Loe, D., Westlake, C., Grant, C., Cole, S., and Deeley, R. (1998) *J. Biol. Chem. 273*, 10733−10740.
12. Bakos, E., Evers, R., Szakacs, G., Tusnady, G., Welker, E., Szabo, K., de, H. M., van, D. L., Borst, P., Varadi, A., and Sarkadi, B. (1998) *J. Biol. Chem. 273*, 32167−32175.
13. Thomas, G. A., Barrand, M. A., Stewart, S., Rabbitts, P. H., Williams, E. D., and Twentyman, P. R. (1994) *Eur. J. Cancer 30A*, 1705−1709.
14. Lorico, A., Rappa, G., Flavell, R. A., and Sartorelli, A. C. (1996) *Cancer Res. 56*, 5351−5355.
15. Lorico, A., Rappa, G., Finch, R. A., Yang, D., Flavell, R. A., and Sartorelli, A. C. (1997) *Cancer Res. 57*, 5238−5242.
16. Wijnholds, J., Evers, R., van, L. M., Mol, C., Zaman, G., Mayer, U., Beijnen, J., van, d. V. M., Krimpenfort, P., and Borst, P. (1997) *Nat. Med. 3*, 1275−1279.
17. Leier, I., Jedlitschky, G., Buchholz, U., Cole, S. P., Deeley, R. G., and Keppler, D. (1994) *J. Biol. Chem. 269*, 27807−27810.
18. Jedlitschky, G., Leier, I., Buchholz, U., Barnouin, K., Kurz, G., and Keppler, D. (1996) *Cancer Res. 56*, 988−994.
19. Loe, D. W., Almquist, K. C., Cole, S. P., and Deeley, R. G. (1996) *J. Biol. Chem. 271*, 9683−9689.
20. Zaman, G. J. R., Flens, M. J., Vanleusden, M. R., Dehaas, M., Mulder, H. S., Lankelma, J., Pinedo, H. M., Scheper, R. J., Baas, F., Broxterman, H. J., and Borst, P. (1994) *Proc. Natl. Acad. Sci. U.S.A. 91*, 8822−8826.
21. Loe, D., Deeley, R., and Cole, S. (1998) *Cancer Res. 58*, 5130−5136.
22. Loe, D. W., Almquist, K. C., Deeley, R. G., and Cole, S. P. (1996) *J. Biol. Chem. 271*, 9675−9682.
23. Nielsen, D., and Shovsgaard, T. (1992) *Biochem. Biophys. Acta 1139*, 169−183.
24. Leier, I., Jedlitschky, G., Buchholz, U., Center, M., Cole, S., Deeley, R., and Keppler, D. (1996) *Biochem. J. 314*, 433−437.
25. Renes, J., de Vries, E. G., Nienhuis, E. F., Jansen, P. L., and Muller, M. (1999) *Br. J. Pharmacol. 126*, 681−688.
26. Daoud, R., Desneves, J., Deady, L. W., Tilley, L., Scheper, R. J., Gros, P., and Georges, E. (2000) *Biochemistry 39*, 6094−6102.
27. Vezmar, M., Deady, L. W., Tilley, L., and Georges, E. (1997) *Biochem. Biophys. Res. Commun. 241*, 104−111.
28. Nare, B., Prichard, R. K., and Georges, E. (1994) *Mol. Pharmacol. 45*, 1145−1152.
29. Ludescher, C., Thaler, J., Drach, D., Drach, J., Spitaler, M., Gattringer, C., Huber, H., and Hofmann, J. (1992) *Br. J. Haematol. 82*, 161−168.
30. Twentyman, P. R., Rhodes, T., and Rayner, S. (1994) *Eur. J. Cancer 30A*, 1360−1369.
31. Shapiro, A., and Ling, V. (1998) *Eur. J. Biochem. 254*, 189−193.
32. Jones, T. R., Zamboni, R., Belley, M., Champion, E., Charette, L., Ford-Hutchison, A. W., Frenette, R., Gauthier, J.-Y., Leger, S., Masson, P., McFarlane, C. S., Piechuta, H., Rokach, J., Williams, H., Young, R. N., DeHaven, R. N., and Pong, S. S. (1989) *Can. J. Physiol. Pharmacol. 67*, 17−28.
33. Lowry, O. H., Rosebrough, N. J., Farr, A. L., and Randall, R. J. (1951) *J. Biol. Chem. 193*.
34. Georges, E., Zhang, J.-T., and V., L. (1991) *J. Cell Physiol. 148*, 479−484.
35. Hipfner, D., Gao, M., Scheffer, G., Scheper, R., Deeley, R., and Cole, S. (1998) *Br. J. Cancer 78*, 1134−1140.
36. Fairbanks, G., Steck, T. L., and Wallach, D. F. H. (1971) *Biochemistry 10*, 2606−2617.
37. Cleveland, D. W., Fischer, S. G., Kirschner, M. W., and Laemmli, U. K. (1977) *J. Biol. Chem. 252*, 1102−1106.
38. Bradley, G., Naik, M., and Ling, V. (1989) *Cancer Res. 49*, 2790−2796.
39. Johnson, L. V., Walsh, M. L., and Chen, L. B. (1980) *Proc. Natl. Acad. Sci. U.S.A. 77*, 990−994.
40. Neyfakh, A. A. (1988) *Exp. Cell Res. 174*, 168−176.
41. Hipfner, D., Almquist, K., Stride, B., Deeley, R., and Cole, S. (1996) *Cancer Res. 56*, 3307−3314.
42. Nare, B., Liu, Z., Prichard, R. K., and Georges, E. (1994) *Biochem. Mol. Pharmacol. 48*, 2215−2222.
43. Greenberger, L. M., Yang, C.-P. H., Gindin, E., and Horwitz, S. B. (1990) *J. Biol. Chem. 265*, 4394−4401.
44. Greenberger, L. M. (1993) *J. Biol. Chem. 268*, 11417−11425.
45. Morris, D. I., Greenberger, L. M., Bruggemann, E. P., Cardarelli, C., Gottesman, M. M., Pastan, I., and Seamon, K. B. (1994) *Mol. Pharmacol. 46*, 329−337.
46. Gros, P., Dhir, R., Croop, J., and Talbot, F. (1991) *Proc. Natl. Acad. Sci. U.S.A. 88*, 7289−7293.
47. Loo, T., and Clarke, D. (1998) *Methods Enzymol. 292*, 480−492.

48. Suzuki, S., and Sugiyama, Y. (2000) *Proc. Am. Assoc. Cancer Res. 41*, 673.
49. Stride, B. D., Cole, S. P. C., and Deeley, R. G. (1999) *J. Biol. Chem. 274*, 22877−22883.
50. Cole, S. P. C., Bharswaj, G., Gerlach, J. H., Mackie, J. E., Grant, C. E., Almquist, K. C., Stewart, A. J., Kurz, E. U., Duncan, A. M. V., and Deeley, R. G. (1992) *Science 258*, 1650−1654.
51. Loe, D. W., Stewart, R. K., Massey, T. E., Deeley, R. G., and Cole, S. P. (1997) *Mol. Pharmacol. 51*, 1034−1041.
52. Vezmar, M., and Georges, E. (1988) *Biochem. Pharmacol. 56*, 733−742.
53. Twentyman, P. R., Rhodes, T., and Rayner, S. (1994) *Eur. J. Cancer 30A*, 1360−1369.
54. Versantvoort, C. H., Rhodes, T., and Twentyman, P. R. (1996) *Br. J. Cancer 74*, 1949−1954.

BI0020574